



Evaluating natural and anthropogenic inputs on the distribution of potentially toxic elements in urban soil of Valdivia, Chile

Daniele Tardani · Francisca Vera · Fernanda Álvarez-Amado · Violeta Tolorza · Juan Pablo Lacassie · Domingo Jullian · Carolina Sepúlveda · Pablo Sánchez-Alfaro · Linda Daniele · Leopoldo Gutiérrez

Received: 25 May 2023 / Accepted: 10 July 2023 / Published online: 25 July 2023
© The Author(s), under exclusive licence to Springer Nature B.V. 2023

Abstract The increasing population in urban areas in the last decades requires an effort to understand the geochemistry of contaminant elements in urban soil. Topsoil plays a crucial role in the exposure of Potentially Toxic Elements (PTEs) to humans through ingestion, dermal contact, and inhalation. In Chile, the last census revealed that 88.6% of people live in cities or towns and only 11.4% in rural areas. This study presents the first systematic geochemical survey of urban soil in the city of Valdivia, in the South of Chile. Topsoil samples (0–10 cm depth) were collected in less disturbed locations within the city at 130 sampling sites using a grid of 0.25 km² squares

covering a total area of approximately 30 km². The concentrations of Al, Fe, Na, Ca, Mg, K, Ti, Be, V, Cr, Mn, Co, Ni, Cu, Zn, As, Mo, Sn, Cd, Se, Pb and Hg were measured. The results showed that high concentrations of Cu, V, Zn and Pb are located mainly in the city's northern area and exceed international soil quality legislation for agricultural use. Data processing comprised plotting of individual spatial distribution maps and the use of a combination of multivariate statistical methods. Hierarchical cluster analysis and principal component analysis identified three element associations. The two element groups V–Al–Ti–Fe–Cr–Co–Mn–Be–Ni and Ca–Na–K–As–Mg are interpreted as a dominant lithological origin related to the most pristine soil conditions in less populated areas. By contrast, the Sn–Pb–Zn–Mo–(Cu–Hg)

Supplementary Information The online version contains supplementary material available at <https://doi.org/10.1007/s10653-023-01687-5>.

D. Tardani · D. Jullian
Instituto de Ciencias de la Ingeniería, Universidad de O'Higgins, Rancagua, Chile

F. Vera (✉) · C. Sepúlveda · P. Sánchez-Alfaro
Facultad de Ciencias, Instituto de Ciencias de la Tierra, Universidad Austral de Chile, Valdivia, Chile
e-mail: francisca.vera01@alumnos.uach.cl

F. Álvarez-Amado
Departamento de Ciencias de la Tierra, Facultad de Ciencias Químicas, Universidad de Concepción, Concepción, Chile

F. Álvarez-Amado · L. Gutiérrez
Water Research Center for Agriculture and Mining – CRHIAM, FONDAP ANID Center, Concepción, Chile

V. Tolorza
Universidad de La Frontera, Temuco, Chile

J. P. Lacassie
Servicio Nacional de Geología y Minería, Dirección Regional de Los Ríos, Valdivia, Chile

L. Daniele
Departamento de Geología, Facultad de Ciencias Físicas y Matemáticas, Universidad de Chile, Santiago, Chile

L. Gutiérrez
Department of Metallurgical Engineering, Universidad de Concepción, Concepción, Chile

association presents a significant correlation with urbanization indicators, including vehicular traffic and industrial activities developed since the end of the nineteenth century in Valdivia.

Keywords Quality control · Cluster analysis · Principal components · Factor scores maps · Health risk assessment · Vehicular traffic

Introduction

Recent studies estimate that more than half of the world's population lives in urban areas, with an expected increase of 68% by 2050 (United Nations, 2019). In Chile, the last census revealed that 88.6% of people live in cities or towns and 11.4% in rural areas (INE, 2018). Therefore, the interest in the distribution and bioavailability of potentially toxic elements (PTEs) in urban soil has significantly increased during the last decades, and many related studies have been conducted worldwide (e.g., Argyraki & Kelepertzis, 2014; Birkle & Rauch, 2000; Binner et al., 2023; Dao et al., 2010; Demetriades & Birke, 2015a, 2015b; Demetriades et al., 2018; Johnson et al., 2011; Konstantinova et al., 2019; Cetin et al., 2023). The contamination of urban soil is an indicator of human exposure to PTEs that could represent a potential health risk (Wong et al., 2006). Moreover, the soil is a crucial route for human exposure to contaminants through ingestion, dermal contact, and inhalation or indirect interactions (soil to air, water, or food chain). In particular, the human population is constantly in direct contact with the shallowest layer of soil (topsoil). This layer is unique as it contains a record of urbanization history. Its chemical composition depends on the natural processes of soil formation and parental rock composition, combined with the anthropogenic activities that have been in operation during its historical development (Demetriades & Birke, 2015a, 2015b). Assessing the distribution and origin of PTEs in urban soil is critical since many health-related problems are linked to the state of the urban environment (Filippelli et al., 2012; Johnson et al., 2011; Thornton, 1990). Identifying PTEs in soil is the first stage for health risk assessment, providing critical knowledge to take concrete actions in reducing the risk to the population.

In Chile, regulations such as Law 19,300 on the overall environmental state regulates compliance of soil quality. State institutions, such as Chile's Agriculture and Livestock Service (SAG), Ministry of the Environment (MMA), and the Chilean Environmental Assessment Service (SEA), are responsible for enforcing compliance with environmental regulations. Meanwhile, Chile's National Geology and Mining Service (SERNAGEOMIN) has conducted geochemical studies in river sediments, mainly in the north and central regions of the country, where mining activities may cause contamination of riverbeds. However, despite the existing laws and parameters to measure the aptitude of soil, no law in Chile currently regulates soil quality. Furthermore, clear threshold concentrations of PTEs in urban and agricultural soils are still lacking. Thus, it becomes critical to conduct studies on the geochemistry of topsoil in urban areas of Chile to evaluate the accumulation of PTEs and its sources in Chilean cities.

During the last 5 years, in Chile, a few studies have assessed the geochemical composition of urban soil in a few cities in the central and northern part of the country, including the capital, Santiago (Aruta et al., 2022; Tume et al., 2016, 2018, 2019, 2021; Valdés Durán et al., 2021). Despite these significant advances, information about the state of urban and agricultural soil in Chile and human exposure to PTEs is still scarce. Furthermore, due to the climatic heterogeneity of the country and the difference in natural and anthropogenic processes between north and south (e.g., mining activities are focused in the semi-arid to arid central and northern parts of Chile, whereas the lumber industry takes place mainly in the rainy south), the origin and distribution of PTEs in urban soil are expected to be different.

The present work aims to determine the concentrations, origin and health risk of PTEs in the urban topsoil of the city of Valdivia, located in the coastal area in the south of the country. The city started its industrial development at the end of the nineteenth century with the arrival of European settlers. In recent years, after the 1960's earthquake, Valdivia has been the object of rapid population growth and city expansion. Valdivia's topsoil provides an excellent case study to explore the distribution and origin of PTEs in a city where different anthropic activities have profoundly modified the natural background during the last three centuries. For this purpose, we present the first

geochemical dataset of topsoil composition of a city in Southern Chile, incorporating major elements such as aluminum (Al), iron (Fe), sodium (Na), calcium (Ca), magnesium (Mg), manganese (Mn), potassium (K), titanium (Ti), and PTEs such as beryllium (Be), vanadium (V), chromium (Cr), cobalt (Co), nickel (Ni), copper (Cu), zinc (Zn), arsenic (As), molybdenum (Mo), tin (Sn), cadmium (Cd), selenium (Se), lead (Pb), and mercury (Hg). The natural and anthropogenic origin of these elements in Valdivia topsoil is evaluated through multivariate statistical methods.

The study area

The city of Valdivia (Fig. 1), located at coordinates 39° 48' S and 73° 14' W, is the capital of the XIV Region in Chile. Valdivia is in continuous population and infrastructure growth, with a current area of

1015.6 km² and a population of 166,080 inhabitants, of which 93.2% belong to the urban and 6.8% to the rural population (INE, 2018). Its main current economic activities are the lumber industries, shipyards, breweries, and paper mills (CONAF, 2016). The climate of Valdivia is characterized as warm-rainy temperate with Mediterranean type influence (Luebert & Plissock, 2006). According to the data from Chile Meteorological Office, the average annual rainfall and temperature is 2310 mm, and 12 °C, respectively. In addition, the contribution of the rivers increases environmental humidity, the average being greater than 80% (Montaldo, 1983).

The main geological units located in the province of Valdivia correspond to a set of igneous, metamorphic, and sedimentary rocks with ages from the Upper Paleozoic to the Holocene and are described in the Valdivia–Corral geological map (Mella et al., 2012). The oldest formation present in the area is the

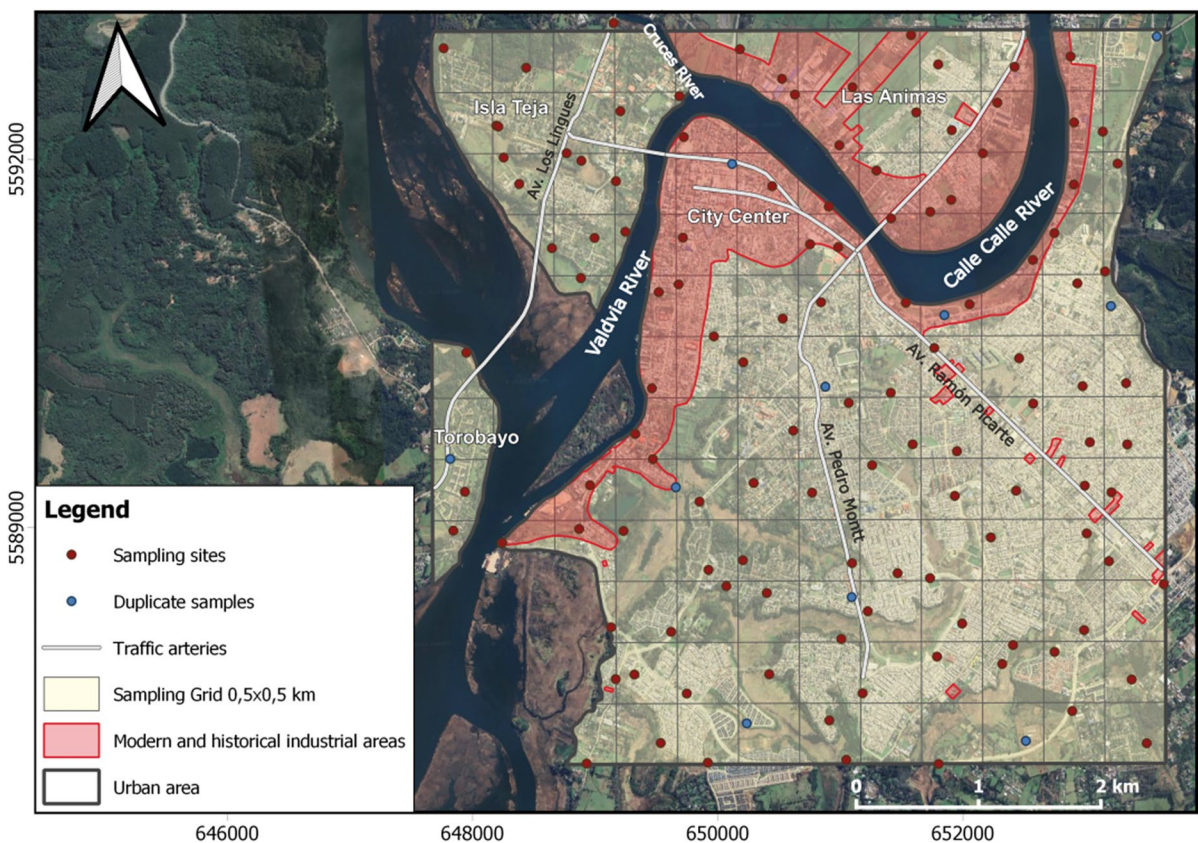


Fig. 1 Google Earth satellite image showing the urban area of Valdivia, the sampling grid and the locations of sampling sites ($n = 130$), as well as the industrial areas and the main traffic arteries of the city

Paleozoic–Triassic metamorphic basement, which belongs to the Bahía Mansa Metamorphic Complex (CMBM), corresponding to mafic schist, amphibolite schist and peridotite. It comprises most of the Coastal Cordillera and Cenozoic sedimentary rocks (Feucker et al., 2014; Juárez et al., 2012). These rocks are covered by Quaternary periglacial, glacial, and fluvial sediments, which filled the sedimentary basins of the Andean foothills. The city of Valdivia is located on the plains of the Calle-Calle, Cruces, and Valdivia rivers, made up of fluvio-estuarine sediments from the last interglacial period, with heights of 13 m above sea level and fluvial sediments that make up the lower terraces, up to 5 m above sea level, of the current riverbeds (Arenas et al., 2005). The fluvio-estuarine sediments are made up of sand, fine sandy gravel, silt, and clay, moderately to weakly consolidated. Depending on the origin of the components, these deposits are divided into two associations of sediments that interbedded laterally (Arenas et al., 2005). The first one is composed of irregular deposits of clay, silt, sand, and a smaller amount of gravel. The sands and other finer materials are mainly composed of fragments of metamorphic rocks and quartz, which indicates that this material would come mainly from the erosion of the CMBM (Arenas et al., 2005). The second one is composed of fine gravel, sand, silty-clay sand, silt, and clay. The fragments correspond mainly to volcanic rocks (basalt and andesite), quartz, magnetite, and weathered rounded pumice. Locally, layers of volcanic lithics occur. In the sand fraction, angular fragments of andesite and basalt and crystals of feldspars, magnetite, olivine, and pyroxene predominate, and to a lesser extent quartz and hornblende (Arenas et al., 2005). The fluvial sediments are composed of well-sorted gravel and coarse sand with a variable proportion of fine material and organic matter. The grains correspond mainly to volcanic (basalt and andesite) and intrusive (granodiorite) rocks. The thickness of these deposits is variable and reaches up to 30–35 m, and the organic matter content increases with proximity to the rivers (Arenas et al., 2005). For the urban area of Valdivia, metamorphic and volcanic rocks are the dominant parent materials, determining the presence of Inceptisols and Andisols (Casanova et al., 2013). Soil substrate consists of gravel deposits with different degrees of weathering, very weathered tuff and metamorphic phyllites and mica schists. Soil thickness varies from thin to moderate, and it is

governed by the extent and intensity of erosion (Casanova et al., 2013).

The urbanization of the city of Valdivia has led to its expansion toward different productive sectors. Its industrial activity has been changing during the last centuries (Fig. 1). During the first half of the nineteenth century, the city of Valdivia was consolidated as a small and underdeveloped city compared to the rest of the country, having numerous river branches and estuaries that crossed the perimeter of the city (Espinoza & Zumelzu, 2016). Subsequently, in 1845, the arrival of European settlers in the area marked a time of industrial development and expansion of the city, filling the estuaries and rivers that crossed Valdivia with landfill material composed of concrete fragments, wood, rock and debris for the construction of buildings and houses (Baessolo and Fuentes, 2011). The industrial development of the city increased with the arrival of the railway in 1899. Shoe factories, tanneries, mills, shipyards, breweries, sugar refineries, paper mills, lumberyards, workshops, and warehouses facilities operated mainly in the center of the city, Las Animas and along the Calle-Calle riverbank (Almonacid, 1995). In 1960, Valdivia was struck by the most powerful earthquake ever recorded (9.4–9.6 Mw), which also triggered a tsunami, land subsidence and floodings. Landscape changes produced a significant migration of the population to the eastern and southeastern sectors of the city, also populating the northern sector of Isla Teja and paralyzing most of the industrial activity (Borsdorf, 2000). In 1988, the expansion of the city began toward traditionally agricultural areas (southern sector) (Espinoza & Zumelzu, 2016), reaching the current urban planning.

Materials and methods

Sampling and chemical analysis

The geochemical survey of the urban soil of Valdivia was carried out between February and May 2021. A sampling grid was established based on the EuroGeoSurvey urban topsoil manual (Demetriades & Birke, 2015a, 2015b), composed of 500×500 m squares (one sample site per 0.25 km²), covering a total area of approximately 30 km² in the urban district of Valdivia (Fig. 1). A combined coverage

method was chosen, based on the combination of systematic sampling (one sample in every square) and an unsystematic method (random points). This approach gave us greater flexibility when defining the sampling points, allowing us to make the necessary adjustments in the field. A total of 130 topsoil samples (VAL_001–VAL_130) were collected mostly in parks, green spaces, and lawns. Also, 10 blind duplicate samples were obtained at points Val_030, Val_040, Val_050, Val_060, Val_070, Val_080, Val_090, Val_100, Val_110 and Val_120 from the same soil mixture of the original sample. The duplicates were labeled with codes from Val_131 to Val_140 and were sent to the laboratory with the other samples.

A patch of urban land was selected within every square where the topsoil was least disturbed. Bare soil or a place with scarce vegetation cover was preferred; in places with vegetation, this layer had to be removed. The sampling depth was determined between 0 and 10 cm, according to the majority of urban topsoil geochemical surveys described in the textbook by Johnson et al. (2011), and subsequently by Demetriades and Birke (2015a, 2015b).

In the field, notes about the surrounding landscape (e.g., topography, presence of outcrops, land use) and nearby anthropogenic activities were recorded. At each sampling point, before collecting the material, the soil patch was cleared with a shovel. Once cleared, a 50×50 cm square was delimited, and another 25×25 cm square was demarcated in the center within the previous one according to the procedure described by Demetriades and Birke (2015a, 2015b). Next, a 10 cm depth hole was dug. The material was extracted from the central hole with a white plastic scoop and homogenized. Approximately 100 g was collected and placed in a clean 16×15 cm ziplock bag after removing roots, coarse clastic material, and garbage through a nylon 1 mm sieve. Soil physicochemical parameters such as temperature and pH were measured in the field using a portable soil tester. Soil characteristics such as granulometry, soil stratification, humidity, abundance of organic matter and clasts > 2 mm were also assessed based on direct observations of the sampled materials. However, this information was not considered in the data elaboration process, although we are aware that it would have been a valuable tool to improve the interpretation of elemental geochemical patterns. After each sampling

point, all the sampling tools were thoroughly cleaned with distilled water and dried using clean paper. After sampling, a scale was placed into the collection point, and several digital photographs were taken.

The samples were dried in a thermostatically controlled oven at 40 °C. Subsequently, they were homogenized, carefully disintegrated with a porcelain mortar, and passed through a 2 mm nylon sieve. Sieved samples were sent to Activation Laboratories Ltd. (Actlabs) in Canada, where they were pulverized to analytical grain size and analyzed by ICP-MS after a hot aqua regia digestion for Al, Fe, Ca, Mg, Ti, Mn, K, Na, P, V, Zn, Cu, Cr, Pb, Ni, Co, As, Sn, Mo, Be and Hg (analytical results are provided in Table S1 of the Supplementary material).

Several certified reference materials (OREAS 45d, OREAS 922, OREAS 907, OREAS 621, OREAS 263, OREAS 130, OREAS 623, OREAS 521) were used to test the analytical method's accuracy (Table S2 of the Supplementary material). The recoveries obtained ranged from 90 to 110% and were considered satisfactory.

Quality control

Based on the analyses of the ten blind duplicate soil samples, analytical precision was estimated by calculating Relative Percent Difference (RPD). RPD was calculated using the following equation:

$$\text{RPD}(\%) = \left| \frac{x_1 - x_2}{\bar{x}} \right| \times 100 \quad (1)$$

where x_1 is the concentration of an element in the original sample, x_2 is the concentration of the same element in the corresponding duplicate and \bar{x} is their average between the two values. The calculated RPD are presented in Table S3 of the Supplementary material. In most cases, RPD values are acceptable, presenting percentage errors lower than 15% for Al, Fe, Ca, Mg, Ti, Mn, K, Na, P, V, Zn, Cu, Cr, Pb, Ni, Co, As, Sn, Mo; Be and Hg. Values above 15% only occurred for Mo, Sn and Hg for samples Val_050 (35% Mo), Val_060 (25% Sn) and Val_080 (29% Hg). These values were kept despite the unsatisfactory precision because high RPD were detected in only one case out of ten, which could be attributed to inadequate homogenization of the samples. Selenium

and Cd had RPD values >20% in most samples, and they were excluded from further statistical treatment.

Health risk assessment

The Human health risk assessment is used to estimate the potential health effects resulting from exposure to chemical substances, whether carcinogenic or non-carcinogenic (Kamunda et al., 2016; US EPA, 2001). These substances can enter the human body through three different routes: oral ingestion, inhalation, and dermal contact. In this study, we focused on evaluating the average daily intakes (ADIs) of heavy metals in adults (both men and women) and children. To perform these calculations, we used the following equations (Li et al., 2020; Praveena et al., 2015; US EPA, 1996).

$$ADI_{\text{ing}} = \frac{C \times \text{IngR} \times \text{EF} \times \text{ED}}{\text{Bw} \times \text{AT}} \times 10^{-6} \quad (2)$$

$$ADI_{\text{inh}} = \frac{C \times \text{InhR} \times \text{EF} \times \text{ED}}{\text{PEF} \times \text{Bw} \times \text{AT}} \quad (3)$$

$$ADI_{\text{dermal}} = \frac{C \times \text{SA} \times \text{AF} \times \text{ABS} \times \text{EF} \times \text{ED}}{\text{Bw} \times \text{AT}} \times 10^{-6} \quad (4)$$

where C is the concentration of the heavy metal in the soil (mg/kg), IngR and InhR are the rates of ingestion and inhalation, respectively in mg/day, EF is the exposure frequency (days/year), ED is the exposure duration (years), Bw is the individual's body weight (kg), AT is the averaging time period (days), PEF is the particle emission factor (mg^3/kg), SA is the exposed skin area (cm^2), AF is the soil adherence factor (mg/cm^2), and ABS is the fraction of applied dose absorbed through the skin.

To calculate the non-carcinogenic risk, the hazard quotient (HQ) was used according to the following equation (US EPA, 1989):

$$HQ = \frac{ADI}{\text{RfD}} \quad (5)$$

where RfD is the reference dose ($\text{mg}/\text{kg}^{-1}/\text{day}^{-1}$), which represents the highest daily dose of a specific metal in a particular exposure pathway that does not produce noticeable effects in an individual over their lifetime (US EPA, 1986). On the other hand, the hazard index (HI) is the result of summing up all the

hazard quotients obtained for individual heavy metals, which indicates the non-carcinogenic effect in the population. It is calculated using the following equation (US EPA, 1989):

$$HI = \sum_{k=1}^n HQ_k = \sum_{k=1}^n \frac{ADI_k}{\text{RfD}_k} \quad (6)$$

When the Hazard Index (HI) is less than 1, it means that the non-carcinogenic risk to human health is negligible. If the HI is greater than 1, it indicates the presence of a non-carcinogenic risk to health, and this risk increases as the HI increases (Li et al., 2020; Qing et al., 2015).

To calculate the carcinogenic risk (CR), the following formula is used (Diami et al., 2016):

$$CR = \sum_{k=1}^n ADI_k SF_k \quad (7)$$

where SF represents the slope factor ($\text{mg}/\text{kg}^{-1} \text{day}^{-1}$)⁻¹. If the carcinogenic risk $CR < 10^{-6}$, the carcinogenic risk can be ignored; when $10^{-6} < CR < 10^{-4}$, the carcinogenic risk is considered acceptable; when $CR > 10^{-4}$, the carcinogenic risk is deemed unacceptable, being a dimensionless index (Wu et al., 2015).

Statistical treatment

Descriptive and univariate statistical parameters were calculated for individual elements using RStudio, through the StatDA library. The statistical distribution of element concentrations was visualized with histograms, boxplots and density traces by using the 'addplot' function. Element associations were determined using multivariate techniques, such as hierarchical cluster analysis (HCA) and principal components analysis (PCA). The Statgraphics Centurion software was used to obtain the hierarchical cluster analysis diagram on normalized data using the squared Euclidean distance method. Ward's method was used as a grouping formula, which occupies the sum of the squared distances to the centers of the groups. The critical level of union for a set of 130 samples was 1.2. For PCA analysis, the main components were distinguished according to the Kaiser criterion (eigenvalues > 1). Factor loads were calculated using the

Varimax rotation method. Elements, with a load component between |0.5| and |1| as the main signal, have been considered to define the components, where the main geochemical association is > 0.5 and the main inverse signal is < -0.5. In addition, we considered secondary signals ranging from |0.3| to |0.5|. More than one element would be expected to repeat per component, as there is also possibly more than one geochemical association per component due to the geochemical signal. This analysis was carried out using the ‘FactoMineR’ library in RStudio, delivering the PCA of the data through graphs of variables of two components, the percentage of explained variance and the amount that would explain 80% of the variance.

Results and discussion

Element concentrations

For elemental concentrations, T and pH, a summary of descriptive statistics, such as maximum, minimum, mean, median, first (Q1) and third (Q3) quartiles, median absolute deviation (MAD) and orders of magnitude, are reported in Table 1. In Fig. 2 and Fig. S7.1 of supplementary material, chemical concentrations of major and trace elements are graphically presented as boxplots, density traces and histograms. Aluminum shows a left-skewed distribution (Fig. 2), while Ca, Na, Zn, Cu, Pb, As, Sn, and Mo display a right-skewed distribution, and Fe, Mg, Ti, Mn, V, Cr, Ni, Co and Be present distributions close to a bell-shape (Fig. 2, Fig. S7.1).

Table 1 Statistical summary of major and trace element concentrations, T and pH of urban soils in Valdivia (N=130)

Elements	U.M	Min	Q1	Median	Q3	Max	MAD*	Order of Magnitude
Al	%	2.1	4.53	6.13	7.43	8.0	1.42	0.573
Fe	%	1.9	3.94	4.61	5.28	7.9	0.675	0.618
Ca	%	0.06	0.17	0.30	0.52	2.0	0.15	1.51
Mg	%	0.09	0.24	0.30	0.36	0.68	0.055	0.878
Ti	%	0.08	0.18	0.23	0.26	0.44	0.04	0.720
Mn	%	0.02	0.05	0.06	0.05	0.11	0.01	0.841
K	%	0.02	0.03	0.05	0.06	0.15	0.02	0.875
Na	%	0.01	0.02	0.028	0.05	0.22	0.01	1.20
V	mg/kg	75	122.00	150	174.00	267	24	0.551
Zn	mg/kg	34	77.45	102	147.00	549	29.3	1.21
Cu	mg/kg	36	59.93	71	85.05	280	11.6	0.893
Cr	mg/kg	23	30.75	34	38.00	58	4	0.402
Pb	mg/kg	7	15.48	22	33.60	199	8.25	1.43
Ni	mg/kg	10.8	16.70	18.4	21.15	35.9	2	0.522
Co	mg/kg	5.3	12.58	14.2	16.63	31.3	2.05	0.771
As	mg/kg	2.4	4.80	6.0	7.83	23	1.5	0.982
Sn	mg/kg	0.62	1.01	1.32	2.53	16.5	0.45	1.43
Mo	mg/kg	0.16	0.49	0.68	0.81	15.8	0.17	1.99
Be	mg/kg	0.3	0.40	0.50	0.60	0.9	0.1	0.477
Hg	mg/kg	0.02	0.06	0.07	0.09	0.5	0.02	1.39
T	°C	11.4	18.9	21.45	25.00	34.7	–	–
pH	–	3.83	5.3	5.675	6.1	7.29	–	–

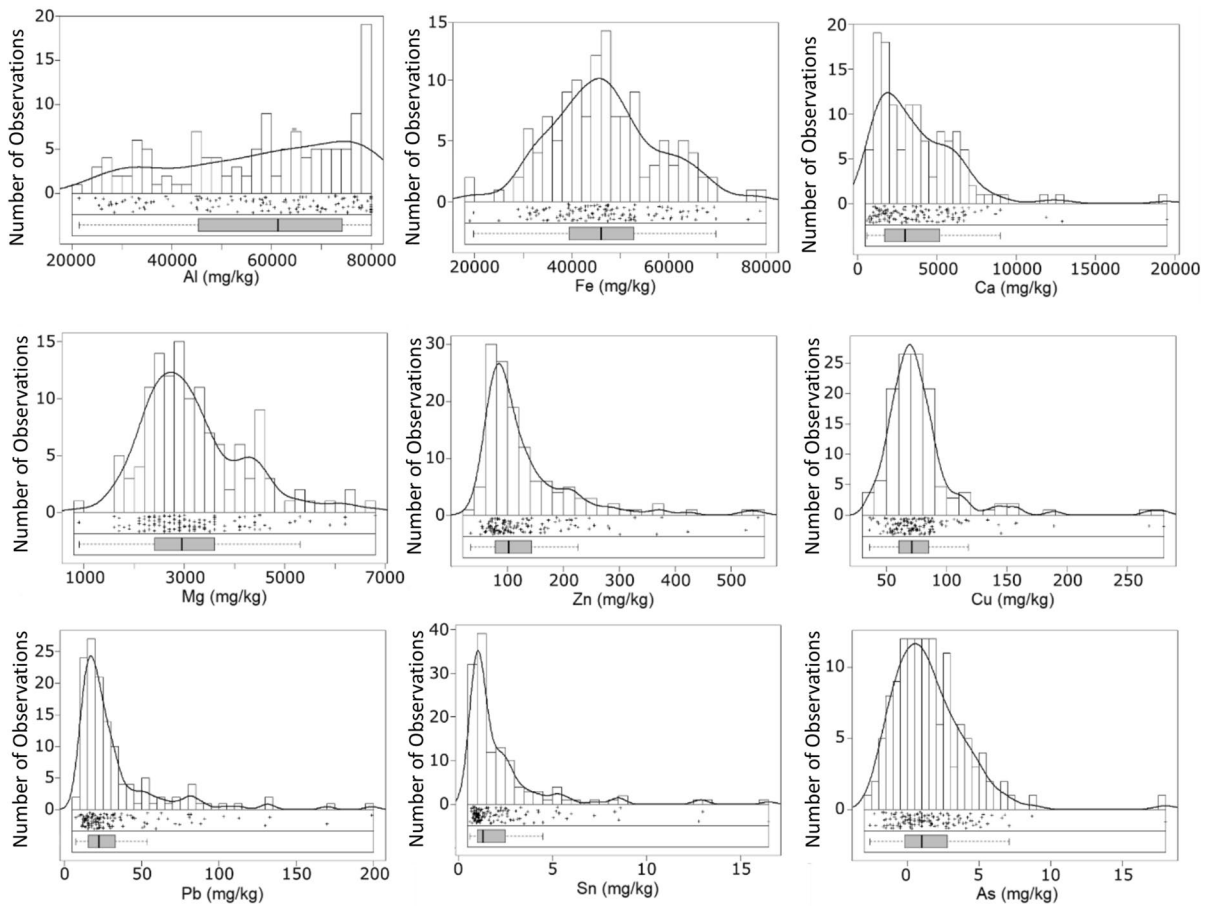


Fig. 2 Combined frequency histogram, density trace and boxplot of hot aqua regia extractable Al, Fe, Ca, Mg, Zn, Cu, Pb, As and Sn concentrations in topsoil samples ($n = 130$), Valdivia, Chile

Comparison with national standards

The Valdivia soil geochemical results were compared with national standards in accordance with the provisions of Chilean law (Article 11 Law 19.300). In this study, we considered the norm of Canada and Germany due to the comparison of variables such use of soils and element concentrations that can be established between the area of study and the selected countries.

Canada establishes thresholds according to land use (agricultural/residential, commercial, industrial), while Germany defines element concentrations according to the types of soils (clay, loamy and sandy).

For this study, we selected agricultural/residential soil from Canada law and clay soil from

Germany law, both of which are similar to Valdivia soil characteristics.

Most of the analyzed element concentrations are below the threshold values instituted by Canadian and German threshold values. The exceptions are for Cu, V, Zn, Pb and As. Copper and V exceed the Canadian thresholds (63 mg/kg Cu and 130 mg/kg V) in more than 90 samples and the German threshold (100 mg/kg Cu) in 14 samples. Zinc exceeds in 20 samples the Canadian and German soil threshold value (200 mg/kg). Lead concentrations in 13 samples exceed the Canadian threshold (70 mg/kg) and 6 samples exceed the German law (100 mg/kg). Arsenic concentrations in 3 samples are above the Canadian threshold (12 mg/kg) and 1 sample exceeds the German threshold (20 mg/kg).

Health risk assessment

The evaluation of carcinogenic and non-carcinogenic risks of the studied elements were obtained for the routes of ingestion, inhalation, and dermal contact, for adults and children. For the hazard quotient (HQ), the ADIs were obtained, using the parameters and RfD detailed in Table S4 and S5 of supplementary material. The HQ values obtained are presented in Table 2. All heavy metals display an HQ less than 1 for the two population groups, indicating an acceptable level of non-carcinogenic risk, according to USEPA (2004). For the total HQ obtained, the elements show the following trend: $\text{Co} > \text{V} > \text{Mn} > \text{As} > \text{Pb} > \text{Cr} > \text{Cu} > \text{Ni} > \text{Zn} > \text{Hg} > \text{Be} > \text{Mo} > \text{Sn}$, both for adults and children. Regarding the HQ values in the three routes of exposure and the two population groups, the following trend is observed: $\text{HQ}_{\text{ing}} > \text{HQ}_{\text{der}} > \text{HQ}_{\text{inh}}$, with the highest Hazard Quotient for oral ingestion.

On the other hand, the calculation of the Hazard Index (HI) estimates the total impact of the non-cancer risk presented by multiple heavy metals (Agency U.E.P., 1986). As shown in Table 2, the total HI values follow the order: $\text{HI}_{\text{ing}} > \text{HI}_{\text{der}} > \text{HI}_{\text{inh}}$ for adults and children. Adults (men and women) show a hazard index of less than 1, which indicates a negligible non-cancer risk to health (Nag et al., 2022). However, in the case of children, a Hazard Index greater than 1 is observed for oral intake (2.81) and for total HI (3). Which would represent a potential non-carcinogenic risk for children, with possible health effects such as allergies, asthma, rashes, cardiovascular, liver and kidney problems due to prolonged contact with elements such as Co and V, or even delays in the development of mental capacities and intellectual disorders due to the ingestion of Pb, among other effects on health (ATSDR, 1992; ASTDR, 2004; ASTDR; 2011).

For the calculation of Cancer Risk (CR) the SF values exposed in Table S5 of supplementary material were used, for oral, inhalation or dermal exposure for heavy metals V, Cr, Pb, Ni, Co, As and Be. The results, presented in Table 3, show total CR values for men, women and children oscillate between 10^{-6} and 10^{-4} (Table 3), presenting an acceptable risk for the urban area of Valdivia. For most of the studied elements were obtained insignificant risk values ($\text{CR} < 10^{-6}$) for adults and children. However, As showed the highest IR value in children

($1,67 \times 10^{-5}$), which indicates an acceptable cancer risk, under control and monitoring conditions (El-Zeiny and Abd El-Hamid 2022; Wei et al., 2015).

Element spatial distribution

Geochemical maps were plotted for the 20 elements analyzed in Valdivia topsoil (Figs. 3, 4, 5, 6 and section S7 of the supplementary material). Vanadium (Fig. 3), Al, Fe, Co, Ti, Mn and Cr present similar patterns (Figs. S7.2, S7.3, S7.4, S7.5, S7.6 and S7.13 in the S7 supplementary material). The highest concentrations (red areas) are observed in the city's peripheral and recently populated parts, corresponding to the south and east areas and in the sectors of Isla Teja and Torobayo. A few spots are also observed in the city center and the Las Animas sector. Moderate concentrations (yellow areas) are detected in the city center and the northwestern and southeastern parts of the city. The lowest values (blue areas) are found in the southern part of Isla Teja, in the central and northern parts of the city, and along the riverbank to the northeast and southwest.

Nickel (Fig. S7.11) and Be (Fig. S7.16) display similar geochemical distributions, with the highest concentrations occurring in the south of the city center and in the city's southern, northeastern, and western parts. Moderate concentrations are in the city center and the city's eastern part. The lowest concentrations are in Isla Teja, in the southwestern part of the city and Torobayo area.

Calcium, Na, Mg and K present analogous patterns (refer to S7 supplementary material). The highest concentrations occur mainly in the areas close to Valdivia and Calle-Calle rivers, in the northern, northeastern, and northwestern parts of the city, and in the area just south of the city center. Few spots are detected in Torobayo and the city's southeastern sector. Moderate concentrations are found in the city center, in Torobayo, in the eastern and western parts of Isla Teja, and in the southern part of the city. The lowest concentrations occur in the southernmost part of the city and the central and northern parts of Isla Teja.

Copper, Pb, and Zn (Figs. 4, 5 and 6), As, Hg, Mo, and Sn, display similar geochemical distributions (Figs. in S7 supplementary material). The highest concentrations are in the city center and southern

Table 2 Values of non-carcinogenic human health risks posed by heavy metals in soil of study area via oral, inhalation and dermal, for adults and children

H	HQ _{ing}				HQ _{inh}				HQ _{der}				HQ _{total}			
	Adult man	Adult women	Children	Children	Adult man	Adult women	Children	Children	Adult man	Adult women	Children	Children	Adult man	Adult women	Children	Children
Mn	4.86E-02	5.47E-02	4.78E-01	4.78E-02	3.66E-03	4.12E-03	1.18E-02	1.18E-02	-	-	-	-	5.23E-02	5.89E-02	4.90E-01	4.90E-01
V	5.15E-02	5.80E-02	5.06E-01	5.06E-02	4.03E-04	4.54E-04	1.30E-03	1.30E-03	8.36E-03	9.41E-03	4.62E-02	4.62E-02	6.02E-02	6.78E-02	5.54E-01	5.54E-01
Zn	1.22E-03	1.38E-03	1.20E-02	1.20E-02	-	-	-	-	2.07E-05	2.33E-05	1.14E-04	1.14E-04	1.24E-03	1.40E-03	1.21E-02	1.21E-02
Cu	4.36E-03	4.91E-03	4.29E-02	4.29E-02	-	-	-	-	3.07E-05	3.46E-05	1.70E-04	1.70E-04	4.39E-03	4.94E-03	4.31E-02	4.31E-02
Cr	1.80E-02	2.03E-02	1.77E-01	1.77E-02	8.45E-05	9.52E-05	2.73E-04	2.73E-04	3.80E-03	4.28E-03	2.10E-02	2.10E-02	2.19E-02	2.46E-02	1.98E-01	1.98E-01
Pb	3.12E-02	3.52E-02	3.07E-01	3.07E-02	-	-	-	-	-	-	-	-	3.12E-02	3.52E-02	3.07E-01	3.07E-01
Ni	1.53E-03	1.72E-03	1.51E-02	1.51E-02	-	-	-	-	2.31E-05	2.60E-05	1.28E-04	1.28E-04	1.55E-03	1.75E-03	1.52E-02	1.52E-02
Co	8.38E-02	9.44E-02	8.24E-01	8.24E-02	6.56E-04	7.39E-04	2.12E-03	2.12E-03	1.86E-02	2.10E-02	1.03E-01	1.03E-01	1.03E-01	1.16E-01	9.29E-01	9.29E-01
As	4.38E-02	4.93E-02	4.31E-01	4.31E-02	6.86E-06	7.72E-06	2.22E-05	2.22E-05	1.85E-04	2.08E-04	1.02E-03	1.02E-03	4.40E-02	4.95E-02	4.32E-01	4.32E-01
Sn	1.40E-05	1.58E-05	1.38E-04	1.38E-04	-	-	-	-	-	-	-	-	1.40E-05	1.58E-05	1.38E-04	1.38E-04
Mo	4.07E-04	4.58E-04	4.00E-03	4.00E-04	1.59E-07	1.79E-07	5.15E-07	5.15E-07	-	-	-	-	4.07E-04	4.58E-04	4.00E-03	4.00E-03
Be	4.39E-04	4.95E-04	4.32E-03	4.32E-04	6.88E-06	7.75E-06	2.22E-05	2.22E-05	1.85E-04	2.09E-04	1.03E-03	1.03E-03	6.32E-04	7.11E-04	5.37E-03	5.37E-03
Hg	6.92E-04	7.80E-04	6.81E-03	6.81E-04	1.08E-07	1.22E-07	3.51E-07	3.51E-07	2.92E-06	3.29E-06	1.62E-05	1.62E-05	6.95E-04	7.83E-04	6.83E-03	6.83E-03
HI	2.86E-01	3.22E-01	2.81E+00	2.81E-01	4.81E-03	5.42E-03	1.56E-02	1.56E-02	3.12E-02	3.52E-02	1.73E-01	1.73E-01	3.22E-01	3.62E-01	3.00E+00	3.00E+00

Table 3 Values of Cancer risk (RC) for via ingestion inhalation, and dermal contact in residential soil, for adults and childrens

CR	CR _{ing}			CR _{inh}			CR _{der}			CR _{total}		
	Adult man	Adult women	Children	Adult man	Adult women	Children	Adult man	Adult women	Children	Adult man	Adult women	Children
V	1.1E-08	1.2E-08	2.2E-08	-	-	-	-	-	-	1.10E-08	1.2E-08	2.2E-08
Cr	2.3E-09	2.60E-09	4.6E-09	1.5E-07	1.7E-07	9.60E-08	-	-	-	1.5E-07	1.70E-07	1E-07
Pb	4.10E-07	4.6E-07	8.1E-07	3.2E-10	3.6E-10	2E-10	-	-	-	4.10E-07	4.6E-07	8.1E-07
Ni	1.12E-07	1.3E-07	2.2E-07	6.2E-09	6.9E-09	4E-09	-	-	-	1.2E-07	1.3E-07	2.2E-07
Co	6.5E-11	7.3E-11	1.3E-10	1.7E-08	1.9E-08	1.1E-08	-	-	-	1.7E-08	1.9E-08	1.1E-08
As	8.4E-06	9.5E-06	1.7E-05	1.3E-09	1.5E-09	8.5E-10	3.6E-08	4E-08	3.9E-08	8.5E-06	9.6E-06	1.7E-05
Be	1.6E-06	1.8E-06	3.2E-06	2.5E-07	2.9E-07	1.6E-07	3.8E-09	4.30E-09	9.2E-11	1.9E-06	2.1E-06	3.3E-06
ΣCR	1.06E-05	1.19E-05	2.08E-05	4.26E-07	4.80E-07	2.76E-07	3.95E-08	4.44E-08	3.95E-08	1.11E-05	1.25E-05	2.12E-05

sectors, in the northern and northeastern parts of the city, along the riverbank to the northeast and southwest and in the eastern part of Isla Teja. These sectors are where Valdivia’s main industrial and commercial activities are located and where the city’s traffic arteries are distributed. Moderate and low concentrations are detected in the recently populated sectors, corresponding to the south of the city, in southern Torobayo and the center and north of Isla Teja.

Multivariate statistical treatment

Multivariate statistical methods are commonly used in urban soil geochemical studies as reliable tools to unfold the relationship among the whole group of elements. The HCA and PCA were performed to determine the anthropogenic and natural origin of element associations (Figs. 7 and 8). The HCA was performed using the pairwise merging method. Through this analysis, a dendrogram was obtained that groups the variables with similar characteristics in the same cluster. According to the agglomeration distance graph, the number of reasonable clusters to be delimited are at 1.2, forming 3 clusters (C1, C2 and C3; Fig. 7). The PCA was used to reduce the number of considered elements, determine their interrelationships, and establish their distribution in the city of Valdivia. Four principal components were identified, accounting for 77% of the total variance (Table S5 and Fig. S7.18 in the S7 supplementary material;). The first two principal components (PC1 and PC2) explain 62% of the total variance and will be used to identify elemental associations (Fig. 8). In Fig. 9 are displayed the distribution maps of factor scores of each sample for PC1 (Fig. 9a) and PC2 (Fig. 9b). Using the HCA and PCA analysis, three elemental associations were distinguished:

Cluster C1 and the PC1 positive loadings refer to the V–Al–Ti–Fe–Cr–Co–Mn–Be–Ni elemental association. It is usually associated with mafic minerals. Their spatial distribution suggests that these elements can be linked with the fluvio-estuarine sediments composing the natural Valdivia soil. According to the factor scores maps, the PC1 positive load distribution (Fig. 9a) is in the southern, western, and northeastern zones of the city and the north of Isla Teja, related to the more peripheral and late populated zones of the city, where most pristine soil conditions can be found. A recent study indicates that the chemical

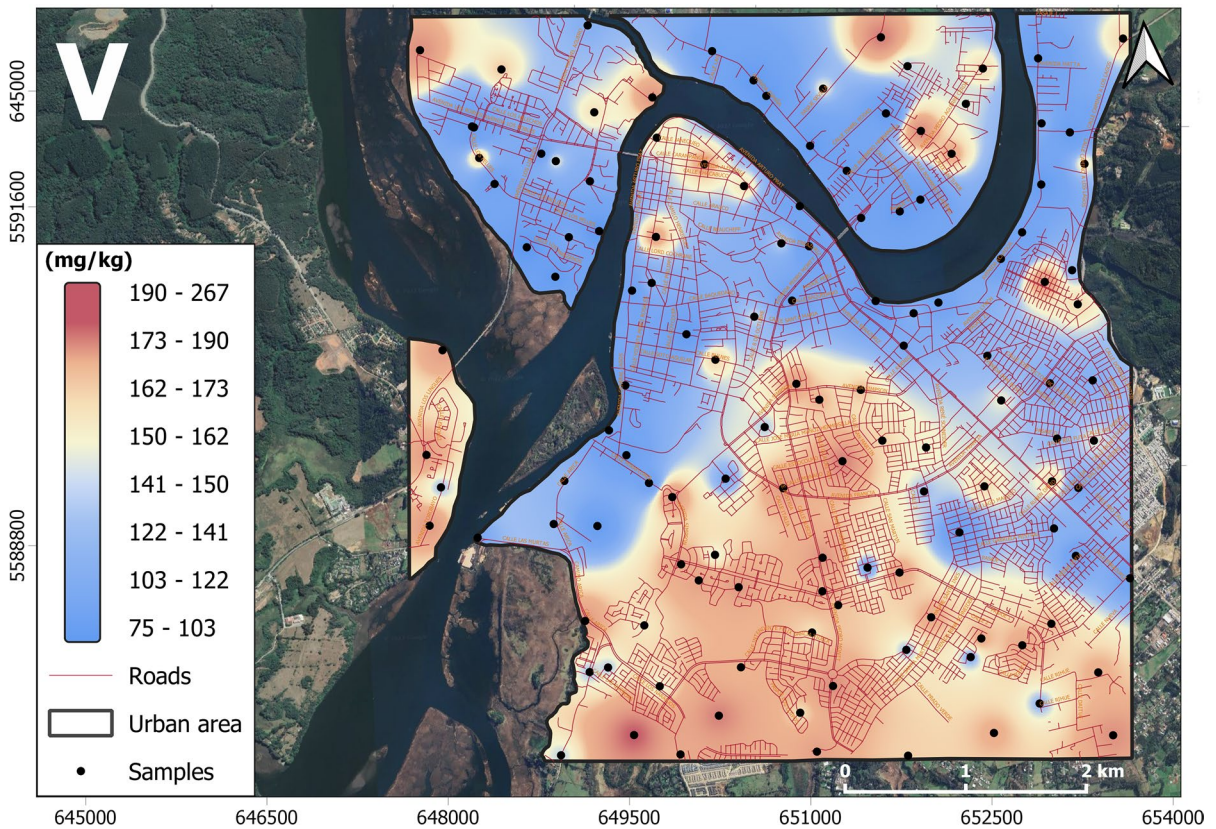


Fig. 3 Spatial distribution of hot aqua regia extractable V concentrations in topsoil samples, Valdivia, Chile

and mineralogical composition of the sediments in the lower part of the basin is controlled by the parent rock, with a predominance of metamorphic basement of the schist or ultrabasic protolith type, while the contribution of volcanic rocks has a more limited dispersion to the east of the Valdivia River basin (Lacassie et al., 2022). Major soil formation products in Inceptisols and Andisols are Al and Fe, which occur in poorly crystalline minerals such as allophane, imogolite and ferrihydrite, and Al-humus complexes (Delmelle, 2015; Nanzyo & Kanno, 2018). Although mineralogical data for Valdivia soil are currently unavailable, the presence of these minerals may explain the high concentrations of Al and Fe (> 8 wt% and 7.9 wt%, respectively). Also, previous studies have highlighted the high concentrations of some elements in volcanic soil, as Al and Fe substituents. For example, Andisols from Japan were found to have relatively high Cr, V, Cu, and Ni contents (Takeda et al., 2004), and those from Hawaii, formed from highly

weathered basaltic lava, have high Co, Cr, Mn, and Ni contents (Burt et al., 2003).

The cluster C2 and the PC1 negative loadings present the Pb–Zn–Sn–Mo–(Cu–Hg) elemental association. These elements are common in hydrothermal deposit minerals, presenting a chalcophile behavior in nature. Elements such as Pb and Sn can be found in relatively high concentrations in soils when their parental rock is an igneous material of intermediate-acid composition, and elements such as Zn, Cu, and Mo are usually associated with minerals of mafic composition such as biotite, pyroxene, and amphibole (Core et al., 2005). The elemental association Sn–Pb–Zn–Mo–(Cu–Hg) is also often related to anthropogenic sources (Binner et al., 2023 and references therein). Lead, Zn and Cu are commonly associated with traffic, railway, and industry (Binner et al., 2023). Tin is associated with urbanization, traffic, industry, and railways, being used mainly for protective coatings (tinning) on steel to prevent corrosion

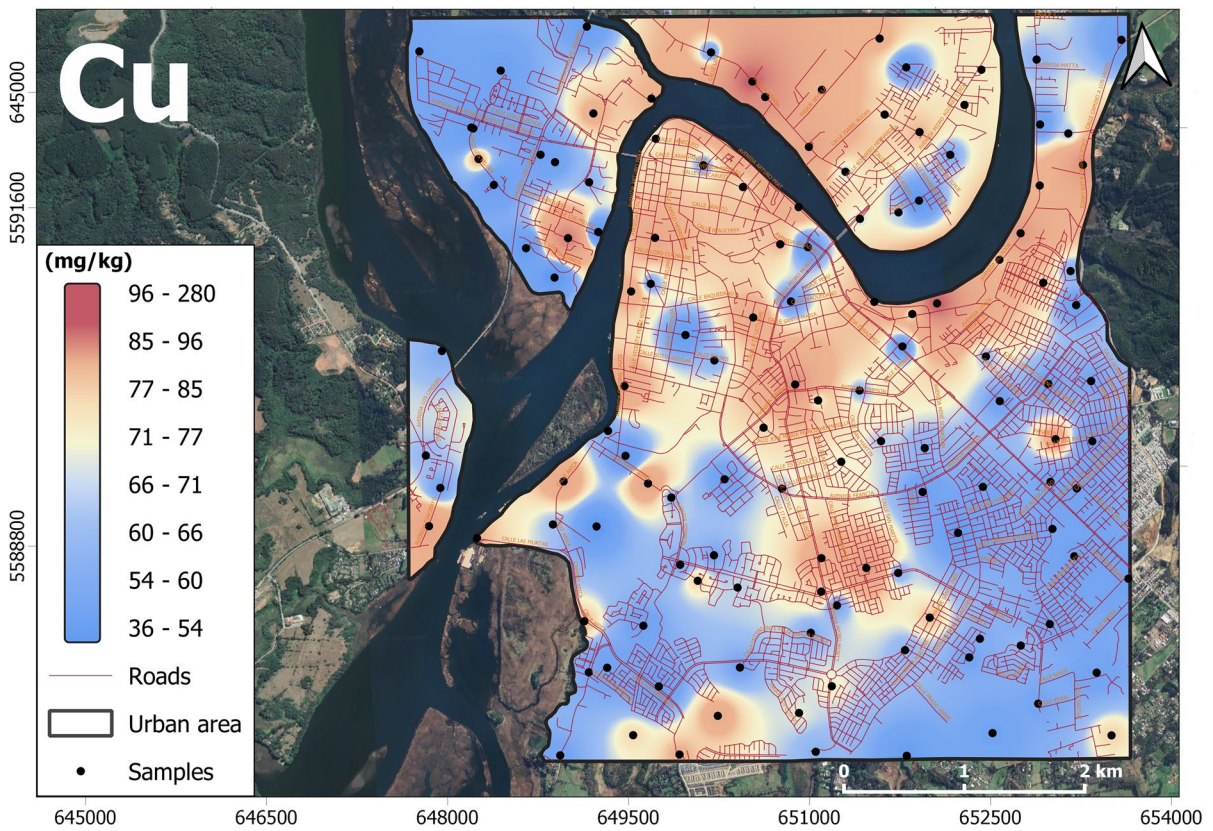


Fig. 4 Spatial distribution of hot aqua regia extractable Cu concentrations in topsoil samples, Valdivia, Chile

and in the manufacture of alloys, some of which are also used in brakes and engine parts in automotive and railway tracks (Stančić et al., 2022). Mercury and Mo may be mainly related to traffic due to the emissions from fossil fuels, catalytic converters, and brakes (Hyun Won et al., 2007; Wong et al., 2021). The distribution map of PC1 factor scores (Fig. 9a) shows that the negative scores correspond with the main traffic arteries (Av. Ramón Picarte, Av. Pedro Montt, Av. Los Lingues; Fig. 1) of the city, and where some of the industrial activities are located. These sectors correspond with the city center, the south of Isla Teja, Torobayo, Las Animas and the southeastern parts of the city. For this association, a prevalent anthropogenic origin is proposed. Vehicular traffic is likely the primary anthropogenic source of these PTEs in Valdivia, with possible input from industrial activities and the railway. Historical urbanization must also be considered as a potential source for these elements, considering that after 1845 Valdivia

began a period of industrial development and urban expansion that led to filling the estuaries and small rivers that crossed Valdivia with landfill material for the construction of buildings and houses in the center and toward the north and southeast (Baessolo and Fuentes, 2011). The landfill material may contribute to the concentration of Pb, Zn, Sn, and Cu in the soil since they are composed of fragments of concrete, wood, rocks, and debris (Barozzi & Lemke, 1966). Also, a minor natural contribution of these elements cannot be discarded. It could be related to fluvio-estuarine sediments, as Cu, Hg, Pb, Zn, Sn, and Mo are potential substituents of Al and Fe in many igneous and metamorphic minerals.

The cluster C3 and the PC2 positive loadings are represented by the Ca–Na–K–As–Mg association. Elements such as K, Ca, and Mg represent essential primary and secondary macronutrients in the soil, which can be found in the parent rock minerals and complex organic molecules (Dhaliwal et al., 2019).

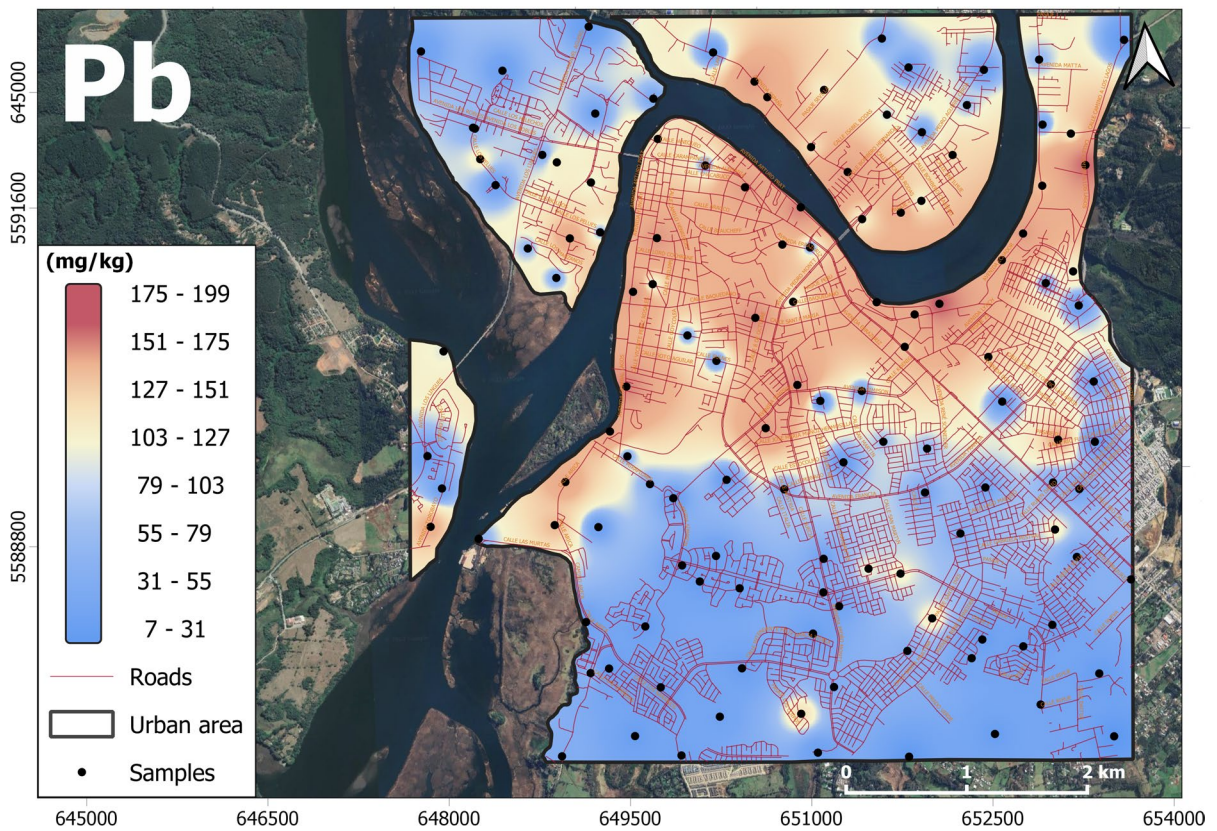


Fig. 5 Spatial distribution of hot aqua regia extractable Pb concentrations in topsoil samples, Valdivia, Chile

Sodium, Ca, and K can be found associated with feldspar and added to the soil through the chemical weathering of parental igneous material. At the same time, in anthropic sources, they are common in fertilizers for agricultural uses. In addition, K has high concentrations in clayey and silty-clayey soils, as well as in phyllosilicates, such as biotite and muscovite (Kumari & Mohan, 2021). Calcium can be found in plagioclase minerals, pyroxenes, amphiboles, olivine, feldspars, limestone, and gypsum, with a range of 0.1–0.2 wt% in non-limestone sourced soil (Nanzyo & Kanno, 2018). Regarding Mg, it is present in mineral phases of olivine, pyroxenes, and amphiboles, also in silicates, biotite, and clay minerals such as chlorite and vermiculite (Nanzyo & Kanno, 2018). Arsenic is found in the environment naturally; its concentrations in igneous rocks are usually below 5 mg/kg, while in sedimentary rocks such as shale and sandstone they can present 12–20 mg/kg, and in metamorphic rocks such as schist and gneiss it can reach up to 18 mg/

kg (Smedley & Kinniburgh, 2002). The map of PC2 positive factor scores (Fig. 9b) shows that all these elements follow a spatial distribution with a more significant influence in the central and northern areas of the city, along the riverbank of the Calle-Calle River, and in the south part of the city. For this association, a lithological origin is proposed. The input of these elements in Valdivia soil would have as main sources the mafic minerals related to stratovolcanoes, volcanic centers, and lava sequences of basaltic and andesitic composition composing the fluvial sediments from Cruces and Calle-Calle River sub-basins, composed of gravel and coarse sand with a variable proportion of organic matter (Mella et al., 2012).

Comparison with other cities in Chile

Throughout Chile, previous studies have been conducted on urban soils in the northern and central regions of the country. Some of these studies show

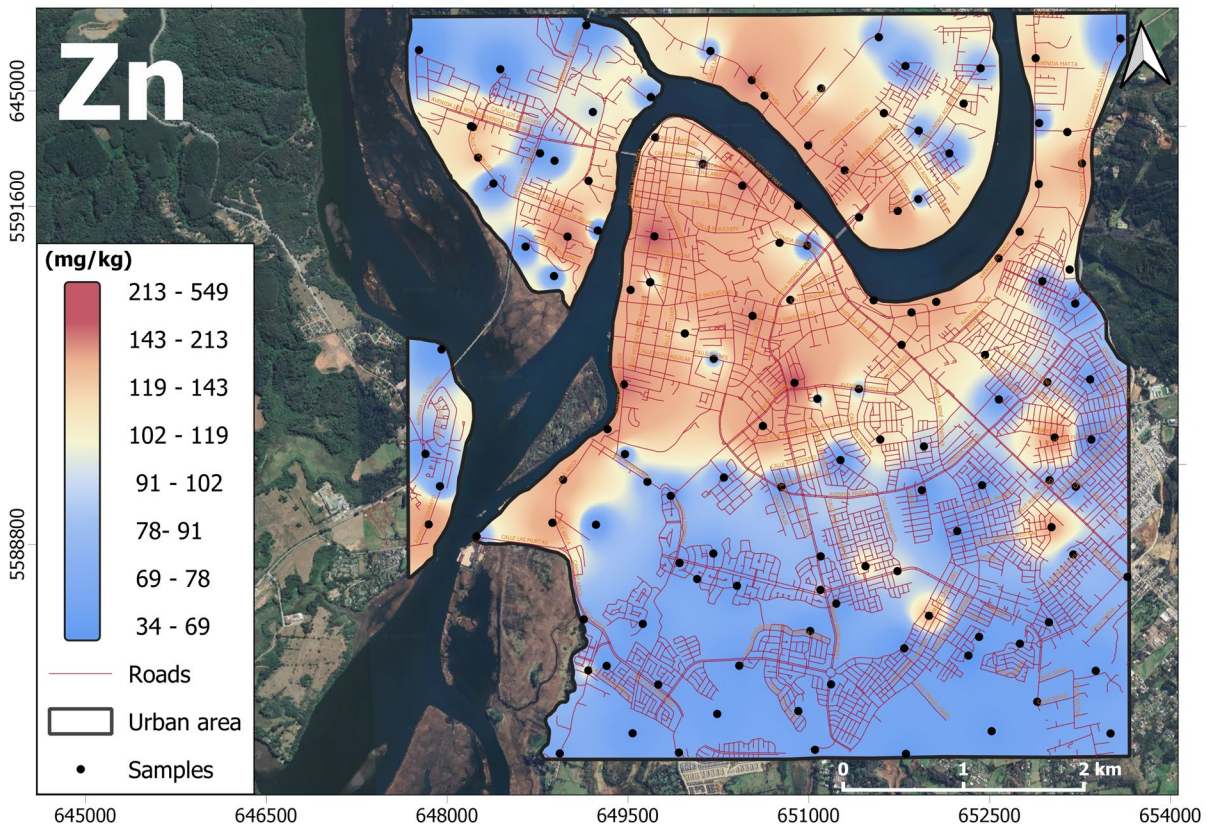
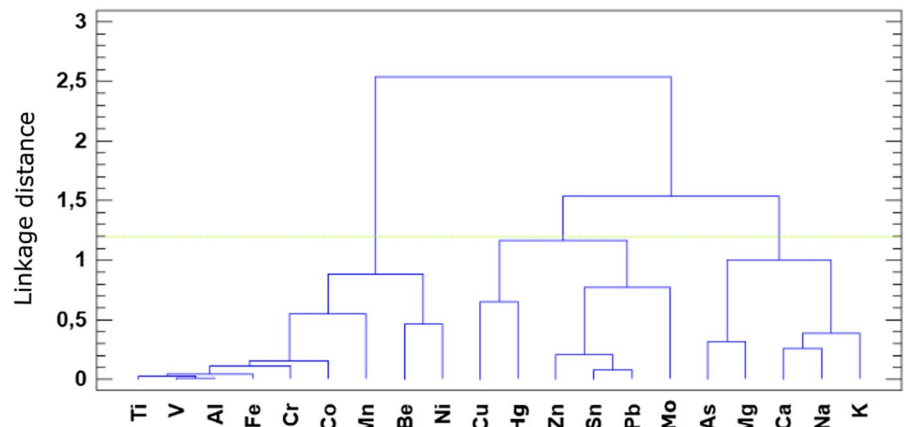


Fig. 6 Spatial distribution of hot aqua extractable Zn concentrations in topsoil samples, Valdivia, Chile

Fig. 7 Hierarchical dendrogram for 20 elements obtained with Ward’s link method. The clusters are **a** V–Al–Ti–Fe–Cr–Co–Mn–Be–Ni, **b** Sn–Pb–Zn–Mo–(Cu–Hg), and **c** Ca–Na–K–As–Mg



similarities in the concentrations of PTEs with those observed in the city of Valdivia, such as in the communes of Arica and Taltal. In Arica (Arica Region), higher concentrations of Cu, Pb, Zn, and As have been observed, which are related to the deposition

of particulate matter from mining operations (Tume et al., 2018). In Taltal (Antofagasta Region), the elevated concentrations of Cu, Pb, Zn, and As are associated with the vehicular traffic emissions, and

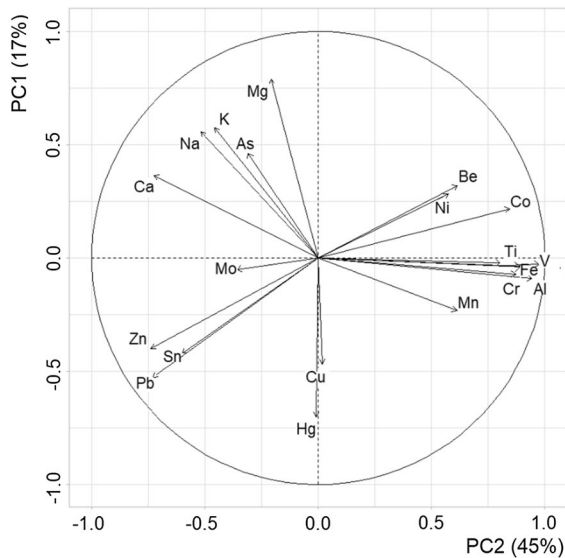


Fig. 8 Explained variance and cumulative variance of principal components (a) and PCA loading plots for Varimax-rotated components (b)

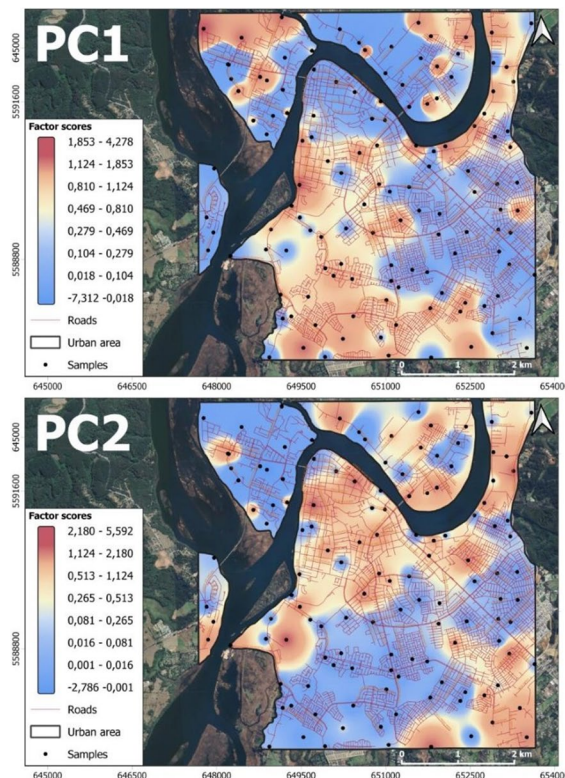


Fig. 9 Spatial distribution of PC1 (a) and PC2 (b) factor scores, Valdivia, Chile

industrial zones (Reyes et al., 2019), as registered in Valdivia.

In central Chile, specifically in the communes of Hualpén and Talcahuano (Biobío Region), the distribution of Cu, Pb, and Zn are associated with the industrial park and vehicular traffic emissions (Tume et al., 2018). However, despite having less industrial development, Valdivia presents higher median concentrations of As, Cu, Zn, Pb, V, and Cr in relation to Hualpén, as well as higher median concentrations of Cu, Pb, and Zn compared to Talcahuano. Also, urban soil studies realized in the commune of Santiago (Metropolitan Region) show high concentrations of Pb, Sb, Sn, Cd, and Zn related to the historic center, motor vehicle traffic, and anthropogenic activities (Adamiec et al., 2016; Aruta et al., 2022).

Concluding remarks

This paper provides the results and discussion of the first systematic geochemical survey of urban soil in the city of Valdivia. Elements such as Cu, V, Zn, and Pb are the PTEs that show the highest concentrations, and most of the analyzed samples present concentrations above Canadian and German environmental legislation.

By calculating the health risk assessment, we conclude that adults show a hazard index of less than 1, indicating a negligible non-carcinogenic risk. In the case of children, a hazard index greater than 1 is observed for oral intake and for total HI, representing a potential non-carcinogenic risk, due to prolonged contact with elements such as Co and V, or Pb.

The element concentrations were subjected to multivariate statistical analysis, and we concluded that relatively clear patterns exist which permit distinguishing between natural and anthropogenic origin. The spatial distribution for individual PTEs vary considerably within the city, reflecting the heterogeneity of both soil and parent rock, in addition to the diversity of the potential anthropogenic sources. The V–Al–Ti–Fe–Cr–Co–Mn–Be–Ni association is mainly of lithological origin. The distribution of these elements is associated with areas that were populated more recently, during the city's expansion in 1988, toward historical agricultural areas that were flooded during the 1960 earthquake. This late populated sector of Valdivia likely coincides with the pristine soil

conditions that originated from the weathering of fluvio-estuarine sediments of the last interglacial period. The Sn–Pb–Zn–Mo–(Cu–Hg) association is assumed to be mainly of anthropogenic origin and is associated with vehicular traffic and to a lesser extent to landfills and industries related to the old part of the city, such as shipyards, mills, and railways, among others. A geogenic contribution for this association may be related to the weathering of mafic minerals, volcanic glasses, and sulfides. Finally, the Ca–Na–K–As–Mg association, distributed mainly in the lower terraces along the riverbank, is related to the fluvial sediments composed mainly of volcanic rocks (basalt and andesite) and organic matter.

This study represents the first step in an urban topsoil risk assessment and a first critical look at sources of contaminants in the city of Valdivia. Vehicular traffic, landfills and industrial activities are possibly the main sources of PTEs, such as Zn, Pb and to a lesser extent Cu, in the topsoil, found in concentrations higher than Canadian and German legislation, could generate a real health risk in the city. Mitigating this risk is mandatory and must be done through local and regional policies that establish clear thresholds for PTEs based on land use, as well as rigorous control over vehicle and industrial emissions and urbanization.

Acknowledgements This paper was partially funded by an academic grant provided by the Universidad Austral de Chile to Daniele Tardani. Additional funding was provided by the projects ANID-Fondecyt #1201219, ANID-Fondecyt #11220777, ANID-Fondecyt #11190864 and ANID-FONDAP #15130015 (CRHIAM). VT thanks to the UFRO Postdoc Grant VRIP20P001. We are grateful to Alecos Demetriades and another anonymous reviewer whose criticisms and suggestions helped to improve this manuscript significantly. The Associate Editor Efstratios Kelepertzis is also thanked for editorial handling.

Author contributions DT contributed to conceptualization, resources, funding acquisition, project administration, methodology, validation, investigation, writing—original draft, and supervision; FV contributed to fieldwork, conceptualization, methodology, writing—original draft, investigation, supervision and figures preparation. FÁ-A contributed to conceptualization, writing—review and editing; VT contributed to resources, writing—review and editing. DJ contributed to writing—review and editing. JPL contributed to validation, writing—review and editing. CS contributed to fieldwork and methodology. PS-A contributed to resources, writing—review and editing. LD contributed to validation, writing—review and editing. LG contributed to resources, writing—review and editing.

Declarations

Conflict of interest The authors declare no conflict of interest.

References

Adamiec, E., Jarosz-Krzeminska, E., & Wieszala, R. (2016). Heavy metals from non-exhaust vehicle emissions in urban and motorway road dusts. *Environmental Monitoring and Assessment*, 188, 369. <https://doi.org/10.1007/s10661-016-5377-1>

Agency for Toxic Substances and Disease Registry (ATSDR). (2011). Division of Toxicology and Environmental Medicine. United States Department of Health and Human Service of EEUU. Public Health Service, p 269.

Agency U.E.P. (1986). Guidelines for the health risk assessment of chemical mixtures. *Federal Register*, 51, 34014–34025.

Almonacid, F. (1995). *Valdivia 1870–1935: Imágenes e historias*. Universidad Austral de Chile.

Arenas, M., Milovic, J., Pérez, Y., Troncoso, R., Behlau, J., Hanisch, J. & Helms, F. (2005). Geología para el ordenamiento territorial: área de Valdivia, Región de Los Lagos. Servicio Nacional de Geología y Minería, Carta Geológica de Chile, Serie Geología Ambiental 8: 71p., 6 mapas escala 1:100.000 y 1 mapa escala 1:25.000.

Argyarak, A., & Kelepertzis, E. (2014). Urban soil geochemistry in Athens, Greece: The importance of local geology in controlling the distribution of potentially harmful trace elements. *Science of the Total Environment*, 482–483(2014), 366–377.

Aruta, A., Albanense, S., Daniele, L., Cannatelli, C., Buscher, J. T., De Vivo, B., Petrik, A., Cicchella, D., & Lima, A. (2022). A new approach to assess the degree of contamination and determine sources and risks related to PTEs in an urban environment: the case study of Santiago (Chile). *Environmental Geochemistry and Health*. <https://doi.org/10.1007/s10653-021-01185-6>

Baessolo, J., & Fuentes, E. (2011). Cronología y catastro de industrias en Valdivia, una mirada a nuestro pasado industrial. El legado alemán y su influencia en la industria. Valdivia conecta. [En línea]. [Consultado 22 de agosto 2022], Disponible en <http://valdivia-conecta.blogspot.com>

Barozzi, R., Lemke, R. (1966). El suelo de fundación de Valdivia. Instituto de Investigaciones Geológicas, Estudios Geotécnicos, N°1,1 mapa escala 1:7.500.

Binner, H., Sullivan, T., Jansen, M. A. K., & McNamara, M. E. (2023). Metals in urban soils of Europe: A systematic review. *Science of the Total Environment*, 854, 158734.

Birke, M., & Rauch, U. (2000). Urban geochemistry: Investigations in the Berlin metropolitan area. *Environmental Geochemistry and Health*, 22, 233–248. <https://doi.org/10.1023/A:1026554308673>

Borsdorf, A. (2000). El desarrollo urbano de valdivia: Estudio de caso en una ciudad mediana. Innsbruck, Austria: Instituto De Geografía De La Universidad De Innsbruck. *Espacio y Desarrollo*, 2000(12), 45–81.

- Burt, R., Wilson, M. A., Mays, M. D., & Lee, C. W. (2003). Major and trace elements of selected Pedons in the USA. *Journal of Environmental Quality*, 32, 2109–2121.
- Casanova, M., Salazar, O., Seguel, O., & Luzio, W. (2013). *The soils of Chile*. World Soils Book Series. <https://doi.org/10.1007/978-94-007-5949-7>
- Cetin, M., Sevik, H., Koc, I., & Zeren Cetin, I. (2023). The change in biocomfort zones in the area of Muğla province in near future due to the global climate change scenarios. *Journal of Thermal Biology*, 112, 103434. <https://doi.org/10.1016/j.jtherbio.2022.103434>
- CONAF. (2016). Plan de protección contra incendios forestales comuna de Valdivia – Región de 1007/s10653-021-01185-6los Ríos
- Core, D. P., Kesler, S. E., Essene, E. J., Dufresne, E. B., Clarke, R., Arms, D. A., & Rivers, M. L. (2005). Copper and zinc in silicate and oxide minerals in igneous rocks from the Bingham: Park City Belt, Utah. *The Canadian Mineralogist*, 43(5), 1781–1796. <https://doi.org/10.2113/gscanmin.43.5.1781>
- Dao, L., Morrison, L., & Zhang, C. (2010). Spatial variation of urban soil geochemistry in a roadside sports ground in Galway, Ireland. *Science of the Total Environment*, 408(2010), 1076–1084.
- Delmelle, P. (2015). *The encyclopedia of volcanoes, volcanic soils*. pp. 1253–1264. <https://doi.org/10.1016/B978-0-12-385938-9.00072-9>
- Demetriades, A., Johnson, C.C. & Birke, M. (Editors) (2018). Urban geochemical mapping: The EuroGeoSurveys geochemistry expert group's URGE project. Special Issue, Journal of Geochemical Exploration, 187, 213 pp. <https://doi.org/10.1016/j.gexplo.2017.10.024>
- Duchauffour, Ph. (1987). Manual de Edafología. Ed. Masson. Barcelona. pp. 214.
- Demetriades, A., & Birke, M. (2015a). *Urban topsoil geochemical mapping manual (URGE II)* (p. 52). EuroGeoSurveys. <https://doi.org/10.5281/zenodo.7319866>
- Demetriades, A., & Birke, M. (2015b). *Urban geochemical mapping manual: sampling, sample preparation, laboratory analysis, quality control check, Statistical processing and map plotting* (p. 162). EuroGeoSurveys. <https://doi.org/10.5281/zenodo.7319969>
- Dhaliwal, S. S., Naresh, R. K., Mandal, A., Singh, R., & Dhaliwal, M. K. (2019). Dynamics and transformations of micronutrients in agricultural soils as influenced by organic matter build-up: A review. *Environmental and Sustainability Indicators*, 1–2, 100007. <https://doi.org/10.1016/j.indic.2019.100007>
- Diami, S. M., Kusin, F. M., & Madzin, Z. (2016). Potential ecological and human health risks of heavy metals in surface soils associated with iron ore mining in Pahang, Malaysia. *Environmental Science and Pollution Research*, 23, 21086–21097. <https://doi.org/10.1007/s11356-016-7314-9>
- El-Zeiny, A. M., & Abd El-Hamid, H. T. (2022). Environmental and human risk assessment of heavy metals at northern Nile Delta region using geostatistical analysis. *The Egyptian Journal of Remote Sensing and Space Science*, 25, 21–35. <https://doi.org/10.1016/j.ejrs.2021.12.005>
- Espinoza, D., & Zumelzu, A. (2016). Valdivia y su evolución post-terremoto 1960: enfoques, factores escalares y condicionantes. *Revista Urbana*, 33, 14–29.
- Feuker, P., V, R. T., Páez, D., Pérez, Y. (2014). Hidrogeología de la cuenca del río Valdivia, Regiones de Los Ríos y de la Araucanía. Servicio Nacional de Geología y Minería. Carta Geológica de Chile, Serie Geología Hidrogeología.
- Filippelli, G. M., Morrison, D., & Cicchella, D. (2012). Urban geochemistry and human health. *Elements*, 8, 439–444.
- Hyun Won, J., Young Park, J., & Gyu, L. T. (2007). Mercury emissions from automobiles using gasoline, diesel, and LPG. *Atmospheric Environment*, 41(35), 7547–7552. <https://doi.org/10.1016/j.atmosenv.2007.05.043>
- Johnson, C. C., Demetriades, A., Locutura, J., & Ottesen, R. T. (Eds.). (2011). *Mapping the chemical environment of urban areas* (p. 616). Wiley-Blackwell, John Wiley & Sons Ltd. <https://doi.org/10.1002/9780470670071>
- Juárez, I., Enguita, P., Cortez, F., Montaner, D., Barrera, J. & Sanhueza, J. F. (2012). Estudio cuencas principales región de los ríos.
- Kamunda, C., Mathuthu, M., & Madhuku, M. (2016). Health risk assessment of heavy metals in soils from Witwatersrand gold mining basin, South Africa. *International Journal of Environmental Research and Public Health*, 13(7), 663. <https://doi.org/10.3390/ijerph13070663>
- Konstantinova, E., Minkinab, T., Sushkovab, S., Konstantinovc, A., Rajputb, V. D., & Sherstnev, A. (2019). Urban soil geochemistry of an intensively developing Siberian city: A case study of Tyumen, Russia. *Journal of Environmental Management*, 239(2019), 366–375.
- Kumari N. & Mohan C. (2021). Chapter (2): Basics of clay minerals and their characteristic properties. In: *Clay and clay minerals*. Intech-Open, London, pp. 1–29. <https://doi.org/10.5772/intechopen.97672>
- Lacassie, J.P., Astudillo, F., Mardones, R., Oliva, P., Castro, R., Quiral, V. & Plaza, F. (2022). Geoquímica y mineralogía de sedimentos fluviales de la cuenca del río Valdivia, regiones de La Araucanía y de Los Ríos, Chile. Servicio Nacional de Geología y Minería, Informe Registrado IR-22–102 (Inédito): 87 p., 5 anexos. Santiago.
- Li, J., Wang, G., Liu, F., Cui, L., & Jiao, Y. (2020). Source apportionment and ecological-health risks assessment of heavy metals in topsoil near a factory, central China. *Exposure and Health*. <https://doi.org/10.1007/s12403-020-00363-8>
- Luebert, L., & Plischoff, P. (2006). *Sinopsis bioclimática y vegetal de Chile* (p. 316). Editorial Universitaria.
- Mella, M., Duhart, P., McDonough, M., Antinao, J., Elgueta, S., & Crignola, P. (2012). Geología del área Valdivia-Corral, Región de Los Ríos. *Servicio Nacional De Geología y Minería. Serie Geología Básica No 137. Mapa Escala, 1, 100.000*.
- Montaldo, P. (1983). Características climáticas de la ciudad de Valdivia y alrededores. *Revista Agro Sur*, 11(2), 138–139.
- Instituto Nacional de Estadísticas (INE). 2018. Censo 2017.
- Nag, R., O'Rourke, S. M., & Cummins, E. (2022). Risk factors and assessment strategies for the evaluation of human or environmental risk from metal(loid)s: A focus on Ireland. *Science of the Total Environment*, 802, 149839. <https://doi.org/10.1016/j.scitotenv.2021.149>
- Nanzyo, M., Kanno, H. (2018). Non-crystalline inorganic constituents of soil. In *Inorganic constituents in soil*. Springer, https://doi.org/10.1007/978-981-13-1214-4_4.

- Praveena, S. M., Ismail, S. N. S., & Aris, A. Z. (2015). Health risk assessment of heavy metal exposure in urban soil from Seri Kembangan (Malaysia). *Arabian Journal of Geosciences*, 8, 9753–9761. <https://doi.org/10.1007/s12517-015-1895-3>
- Qing, X., Yutong, Z., & Shenggao, L. (2015). Assessment of heavy metal pollution and human health risk in urban soils of steel industrial city (Anshan), Liaoning, North-east China. *Ecotoxicology and Environmental Safety*, 120, 377–385. <https://doi.org/10.1016/j.ecoenv.2015.06.019>
- Reyes, A., Thiombane, M., Panico, A., Daniele, L., Lima, A., Di Bonito, M., & De Vivo, B. (2019). Source patterns of potentially toxic elements (PTEs) and mining activity contamination level in soils of Taltal city (northern Chile). *Environmental Geochemistry and Health*. <https://doi.org/10.1007/s10653-019-00404-5>
- Smedley, P., & Kinniburgh, D. (2002). A review of the source, behaviour and distribution of arsenic in natural waters. *Applied Geochemistry*, 17, 517–568.
- Stančić, Z., Fiket, Ž., & Vuger, A. (2022). Tin and Antimony as soil pollutants along railway lines: A Case study from north-western Croatia. *Environments*, 9, 10. <https://doi.org/10.3390/environments9010010>
- Takeda, A., Kimura, K., & Yamasaki, S. (2004). Analysis of 57 elements in Japanese soils, with special reference to soil group and agricultural use. *Geoderma*, 119(3–4), 291–307. <https://doi.org/10.1016/j.geoderma.2003.08.006>
- Thornton, I. (1990). Soil contamination in urban areas. *Palaeogeography, Palaeoclimatology, Palaeoecology (global and Planetary Change Section)*, 82(1990), 121–140.
- Tume, P., González, E., King, R., Monsalve, V., Roca, N., & Bech, J. (2018). Spatial distribution of potentially harmful elements in urban soils, city of Talcahuano. *Chile. Journal of Geochemical Exploration*, 184(2018), 333–344.
- Tume, P., González, E., Reyes, F., Fuentes, J. P., Roca, N., Bech, J., & Medina, G. (2019). Sources analysis and health risk assessment of trace elements in urban soils of Hualpen, Chile. *CATENA*, 175, 304–316.
- Tume, P., Roca, N., Rubio, R., King, R., & Bech, J. (2016). An assessment of the potentially hazardous element contamination in urban soils of Arica. *Chile. Journal of Geochemical Exploration*. <https://doi.org/10.1016/j.gexplo.2016.09.011>
- Tume, P., Acevedo, V., Roca, N., Ferraro, F. X., & Bech, J. (2021). Potentially toxic elements concentrations in schoolyard soils in the city of Coronel, Chile. *Environmental Geochemistry and Health*. <https://doi.org/10.1007/s10653-021-00909-y>
- United States Environmental Protection Agency (USEPA). (1986). Quality criteria for water. United States Environmental Protection Agency office of Water Regulations and Standards. DC, 20460.
- United States Environmental Protection Agency (USEPA). (1989). Risk assessment guidance for superfund volume 1: Human health evaluation manual (Part A); Office of Emergency and Remedial Response.
- United States Environmental Protection Agency (U.S. EPA). (1996). Soil screening guidance: Technical background document. Superfund IUS EPA
- United States Environmental Protection Agency (U.S. EPA). (2001). Toxics release inventory: public data release report. Retrieved June 25, 2023, from www.epa.gov/tri/tridata/tri01.
- United States Environmental Protection Agency (U.S. EPA). (2023). Regional Screening Levels (RSLs): Generic tables: Resident soil. Retrieved June 24, 2023, from <https://www.epa.gov/risk/regional-screening-levels-rsls-generic-tables>.
- United Nations, Department of Economic and Social Affairs, Population Division. (2019). *World urbanization prospects: The 2018 revision (ST/ESA/SER.A/420)*. United Nations.
- United States Environmental Protection Agency (USEPA). (2004). *Risk assessment guidance for superfund volume I: Human health evaluation manual (Part E, supplemental guidance for dermal risk assessment)*. USEPA.
- Valdés Durán, A., Aliaga, G., Ceckart, C., Karas, C., Dante, C., & Nario, A. (2021). The environmental geochemical baseline, background and sources of metal and metalloids present in urban, periurban and rural soils in the O'Higgins region, Chile. *Environmental Geochemistry and Health*. <https://doi.org/10.1007/s10653-021-01098-4>
- Wei, X., Gao, B., Wang, P., Zhou, H., & Lu, J. (2015). Pollution characteristics and health risk assessment of heavy metals in street dusts from different functional reasons Beijing, China. *Ecotoxicology and Environmental Safety*, 112, 186–192.
- Wong, C. S. C., Li, X., & Thornton, I. (2006). Urban environmental geochemistry of trace metals. *Environmental Pollution*, 142(2006), 1–16.
- Wong, M. Y., Rathod, S. D., Marino, R., Li, L., Howarth, R. W., Alastuey, A., et al. (2021). Anthropogenic perturbations to the atmospheric molybdenum cycle. *Global Biogeochemical Cycles*, 35, e2020GB006787. <https://doi.org/10.1029/2020GB006787>
- Wu, S., Peng, S., Zhang, X., Wu, D., Luo, W., Zhang, T., Zhou, S., Yang, G., Wan, H., & Wu, L. (2015). Levels and health risk assessments of heavy metals in urban soils in Dongguan, China. *Journal of Geochemical Exploration*, 148, 71–78. <https://doi.org/10.1016/j.gexplo.2014.08.009>

Publisher's Note Springer Nature remains neutral with regard to jurisdictional claims in published maps and institutional affiliations.

Springer Nature or its licensor (e.g. a society or other partner) holds exclusive rights to this article under a publishing agreement with the author(s) or other rightsholder(s); author self-archiving of the accepted manuscript version of this article is solely governed by the terms of such publishing agreement and applicable law.